Received: 6 February 2022 | Revised: 2 June 2022 | Accepted: 23 June 2022

DOI: 10.1002/pen.26078

RESEARCH ARTICLE

POLYMER ENGINEERING AND SCIENCE WILEY

The absolute heat capacity of polymer grafted nanoparticles using fast scanning calorimetry*

Nazam Sakib[1] | **Yung P. Koh**[1,2] | **Sindee L. Simon**[2]

[1]Department of Chemical Engineering, Texas Tech University, Lubbock, Texas, USA

[2]Department of Chemical and Biomolecular Engineering, North Carolina State University, Raleigh, North Carolina, USA

Correspondence
Sindee L. Simon, Department of Chemical and Biomolecular Engineering, North Carolina State University, Raleigh, NC, 27695 USA.
Email: slsimon@ncsu.edu

Funding information
National Science Foundation, Grant/Award Numbers: DMR-2141221, DMR-2004960

*Gregory B. McKenna Virtual Issue

Abstract

The absolute heat capacity of a matrix-free polystyrene grafted silica nanocomposite system is investigated using ultrafast Flash differential scanning calorimetry (Flash DSC) and compared to results for a neat polystyrene sample of similar molecular weight. The heat capacity of the polymer in the nanocomposite is 8% lower than that of the neat polystyrene. In addition, the step change in heat capacity at the glass transition T_g is 15% lower, indicating a 2 nm-thick immobile layer of polymer around the nanoparticles. There is neither an increase in the nanocomposite heat capacity towards that of the neat material nor any additional ΔC_p steps, indicating that the glassy layer around the nanoparticles remains immobile up to 300°C. In addition to the analysis of the absolute heat capacity, the dynamic temperature gradient in the Flash DSC sample increases linearly with increasing rate of measurement, whereas the noise in the heat capacity data increases linearly with the reciprocal of the scanning rate; the optimum rate for measurements lies between 300 and 1000 K/s for the samples studied here and will depend on the sample thickness.

KEYWORDS

absolute heat capacity, fast scanning Chip calorimetry, glass transition, nanocomposites, polystyrene

1 | INTRODUCTION

The concept of the addition of nanoparticles, either bare or polymer-grafted, in a polymer matrix to tune the mechanical properties is well established.[1–10] The formation of an interfacial layer around the nanoparticles in the resulting nanocomposite has also attracted much attention, and a number of computational and experimental studies[11–77] have attempted to capture the thickness and the dynamics of the interfacial layer and its impact on nanocomposite properties using differential scanning calorimetry (DSC),[14,23,25,27,28,32,34–54,69,70,72–74] broadband dielectric spectroscopy (BDS),[23–25,27,28,32,37–44,46–48,54–60,70] small-angle neutron scattering (SANS),[16,31,49,61–65] nuclear magnetic resonance (NMR),[43,49,58,63–67] rheology[34,40,45,51,65,68,69,71] and other methods.[35,39,47] We previously reported[69] the presence of an immobile glassy layer around the nanoparticles in matrix-free polystyrene grafted nanocomposites based on absolute heat capacity measurements in which a reduction in the step change of absolute heat capacity (ΔC_p) at the glass transition temperature (T_g) was observed for matrix-free grafted systems.

The reduction was interpreted as being proportional to the fraction of the grafted chain segments not undergoing the glass transition leading to a thermally arrested layer. The thickness of the immobilized layer was determined to be ~ 2 nm and approximately twice the thickness as for systems where the polymer is simply blended with the nanoparticles.[69] A "dead" or immobile interfacial layer that does not contribute to the glass transition response has been reported for both conventional nanocomposite systems composed of blends of chains and nanoparticles,[40,45,52,54,72–74] as well as for another grafted system where polydimethylsiloxane (PDMS) chains are tethered to silica nanoparticles.[32] On the other hand, a broadening of the calorimetric T_g or a slower, but not an immobile, interfacial region has been reported in a number of conventional nancomposites[14,18,27,28,41,42,46,54,60] and grafted systems,[25,35] most of which are strongly interacting systems. In some of these works,[14,54] however, the interfacial relaxation is supposedly observed as a second tan δ peak above T_g in dynamic mechanical analysis, but others have argued that this interpretation is incorrect and that the higher temperature peak should be attributed due to a suppression of terminal flow.[51] Importantly, a distinction should be made between grafted systems, where the interfacial slowing down is attributed to the stretching of grafted chains at the interface,[25] and conventional nanocomposites in which the slowing down for strongly interacting polymer/nanoparticle systems is related to the adsorption of "bound" chains onto the nanoparticle.[16,25,26,36,46] In such conventional systems, there is often a broadening of the calorimetric T_g and a reduction in ΔC_p that is recovered at higher temperatures, indicating that the slow interface is not immobile.[27,28,36,46] The question that we want to examine here is whether the heat capacity in our matrix-free grafted polystyrene sample also recovers the full neat value of ΔC_p at high temperature and whether a second calorimetric glass transition exists associated with the interface. To do this, we would like to extend the experimental temperature window of our calorimetric experiments, but a major issue in performing thermal analysis of polymeric materials at high temperatures is the increasing tendency of polymers to degrade at temperatures higher than 200°C even under N_2 atmosphere. In the case of polystyrene, nonoxidative thermal degradation has been found to occur at temperatures as low as 230°C for slow heating under vacuum.[78] For this reason, coupled with the typically long measurement times required to obtain absolute heat capacity from conventional step-scan and adiabatic calorimetry, reports of the absolute heat capacity of polymeric materials at high temperatures are rare.[79–81]

The development of nanocalorimeters, such as the Flash differential scanning calorimeter, with their ability to perform rapid measurements allow access to the thermal properties of materials in a higher temperature range. For example, the melting of silk nanofibers was investigated by heating the material up to temperatures 200 K above their nominal degradation temperature at a rate of 2000 K/s.[82,83] Here, we propose the use of the Flash DSC, for the first time to the best of our knowledge, to obtain the absolute heat capacity of matrix-free grafted polymer nanocomposites, to over 200 K above the nominal T_g to determine the presence of additional relaxations at high temperature.

2 | METHODOLOGY

2.1 | Materials

The polymer nanocomposite (PNC) studied in this work is composed of grafted polystyrene chains of 35 kg/mole (M_w) with a polydispersity (PDI) of 1.4 on silica nanoparticles of 12 nm diameter with a graft density of 0.35 chains/nm^2. The synthesis of the nanocomposite is described elsewhere.[69] The silica content of the sample is 20% as determined using thermogravimetric analysis (TGA). A polystyrene (PS) purchased from Polymer Source Inc. is used to compare behavior without nanoparticles; the neat PS has $M_w = 37.8$ kg/mol with PDI = 1.08.

2.2 | Flash differential scanning calorimeter

A Mettler Toldeo Flash DSC1 equipped with a freon cooler and nitrogen purge is used to measure the heat capacity and the glass transition temperature of the samples. The samples are first dissolved in toluene to prepare solutions for spincoating, using 35 wt% and 20 wt% solutions for the nanocomposite and neat samples, respectively. Spin coating onto plasma-treated silicon wafers is performed using an SCS spincoater Model P6700 series coater operated at 2000 rpm, and the resulting film thicknesses, as measured by AFM, were 2.2 and 1.2 μm for the nanocomposite and neat polystyrene, respectively. The films are dried under vacuum overnight to remove residual solvent. Sample size is 360 ± 10 ng for the nanocomposite film and 392 ± 22 ng for the neat film, as determined from the absolute heat capacity and ΔC_p values at T_g as described in a subsequent paragraph, and these samples are transferred onto the heating area of the flash chip using a deer hair.

The absolute heat capacity is measured by performing Flash differential scanning calorimeter (Flash DSC) runs at 600 K/s from 30°C to 190°C at 600 K/s after cooling at the same rate, and then scanning to higher and higher

temperatures in 20°C increments until the upper-temperature limit is 330°C. The sample masses and absolute heat capacities are determined using the following procedure[84]: first, a symmetry analysis[82] is performed on the raw cooling and heating scans, both performed at 600 K/s, for both the empty and the sample chip, and the symmetry line is obtained by averaging the heat flows obtained on cooling and heating away from any transitions (i.e., the symmetry line is obtained in the glassy and liquid states away from T_g and these segments are connected to give symmetry line in the T_g region). The symmetry line is then subtracted from the raw heat flow data to calculate the symmetry-corrected heat flow values. Subtracting the symmetry-corrected empty chip heat flow from that of the sample gives the symmetry-corrected and addenda-corrected heat flow of the sample. The corrected heat flow data is used to obtain the sample by matching the heat capacity with that obtained in our previous study[69] using step-scan DSC:

$$C_p = \frac{\dot{Q}_{meas}}{m\beta} \quad (1)$$

where $\dot{Q}_{meas}$ is the measured heat flow, β is the experimental heating rate, and C_p is the absolute heat capacity.[69] The sample masses are obtained three ways: from separate analyses of limited data in liquid and glassy regimes, as well as from the step change in heat capacity at T_g (ΔC_p). These three methodologies agree within 10% of one another verifying the consistency of the analyses performed. The same symmetry analysis is also performed for consecutive cooling and heating scans at rates of 2000, 1000, 300, and 100 K/s (with equal cooling and heating rates) from 60°C to an upper temperature as high as 315°C, which depends on the scan rate, to further ensure the efficacy of the symmetry analysis to account for heat losses associated with different cooling/heating rate pair. Recent work by Quick et al. compared the correction of heat losses by the symmetry analysis and by a slow cooling methodology and concluded that the consistency between the two lends credence to their use.[85]

The glass transition temperature (T_g) is measured as a function of the cooling rate for rates ranging from 1000 to 0.1 K/s. After cooling from 190°C to 30°C at the given rate, the sample is heated to 190°C at 600 K/s. The limiting fictive temperature (T_f'), which is equivalent to T_g within 1 K,[86] is calculated using Moynihan's method as shown below in Equation (2):

$$\int_{T_f'}^{T>T_g} (C_{pl} - C_{pg})\,dT = \int_{T<T_g}^{T>T_g} (C_p - C_{pg})\,dT \quad (2)$$

where C_{pl} and C_{pg} are the absolute heat capacities in liquid and glassy states, respectively. A dynamic correction of the glass transition temperature is performed following the method proposed by Schawe J. E. K.[87] by cooling and heating the material at the same rates. A correction for a static thermal gradient is not needed since our sample thicknesses are well below 10 μm and, thus, the static thermal gradient is anticipated to be insignificant.[87]

The temperature calibration of the chip is performed using nonadecane (Acros Organics, 99%), phenanthrene (ChemScene, 98%), and pyrene (Sigma Aldrich, 98%), whose melting points are 30.6, 97.0, and 148.5°C, respectively, with an error of ±0.1°C determined using the indium standard, based on conventional DSC results performed on heating at 10 K/min in a Perkin Elmer DSC1 equipped with an ethylene glycol cooler and N_2 purge. The standards are then placed on the Flash DSC chip and melted upon heating at 600 K/s, the same rate as for our T_g measurements. The difference between the onset of melting measured using the conventional and the Flash DSC are then plotted as a function of the absolute melting point obtained from the conventional DSC. The best linear fit is taken as the temperature correction, with an average absolute error of ±0.3°C for the chip used for PNC and ±0.9°C for the chip used for PS. A secondary temperature correction is also performed to compensate for any error resulting from the surface coverage of the calibrants on the flash chip by matching the T_g obtained on cooling at 0.167 K/s in flash to that obtained on cooling at 10 K/min (0.167 K/s) in conventional DSC; this correction is 1.5 and 1.8 K for PS and PNC, respectively.[69]

3 | RESULTS

The absolute heat capacity of the neat polystyrene PS from the Flash DSC data are plotted in Figure 1 (left) as a function of temperature. Also shown in the same plot is the absolute heat capacity of the same material measured using the step-scan method from our previous study,[69] as well as the C_p data available in literature.[80,81] The absolute heat capacity of the neat polystyrene obtained from Flash DSC on cooling and on heating agrees with one another in both the glassy and the liquid regime. The small enthalpic overshoot present on heating is not observed on cooling, as expected. Also shown in Figure 1 (left) are the two data sets in the literature that go above 300°C for polystyrene. Our data agree well with the literature data in the glassy regime with a deviation of less than 1% from Abu-Isa and Dole's adiabatic calorimeter results,[80] whereas in the liquid state, our data are 5% higher than theirs at 150°C and 3% lower than the data

from Bares and Wunderlich.[81] The scatter observed at temperatures on or beyond 300°C is due to performing only one run up to the highest experimental temperature and lack of averaging thereof. In the high-temperature regime, at temperatures above 150°C, although our data lie between the two data sets reported in the literature, they do appear to flatten slightly above 250°C. We note that Quick et al. also observed a flattening of the temperature-dependent heat capacity for lead, which was not consistent with the literature value, albeit above ~150°C; although more work is needed, the implication may be that an additional correction (beyond the symmetry correction) is needed at high temperatures to obtain accurate C_p values. In order to determine whether our result depended on the rate of measurement, we obtained absolute C_p from equal cooling/heating pair experiments for rates from 2000 to 100 K/s, as shown on the right. The absolute C_p in the glassy and in the liquid regime superpose convincingly with the largest deviation for the slowest cooling/heating rate run of 100 K/s due to an increase in noise (as discussed later). The good superposition indicates that irrespective of the selection of the cooling/heating pair for the symmetry analysis, the absolute heat capacities flatten off with increasing temperature. Moreover, to rule out the possibility of sample degradation, the cooling/heating pair of 600 K/s is repeated right after the 100 K/s pair, also plotted in Figure 1 (right), which shows excellent superposition (within 0.2%) with the absolute heat capacity values obtained in the previous runs.

The absolute heat capacity data obtained for the nanocomposite PNC are plotted with respect to temperature in Figure 2 (left), with data shown after subtracting the silica contribution to C_p using the Shomate equation in the NIST database[88]; in other words, the data shown in Figure 2 are for the polymer only and are normalized per gram polymer:

$$C_{p,PS} = \frac{1}{w_{PS}}\left(C_{p,total} - w_{Si}C_{p,Si}\right) \quad (3)$$

where $C_{p,i}$ and w_i are the heat capacity and weight fraction of component i, where i is polystyrene (PS), silica (Si), or the total heat capacity for the nanocomposite system. The absolute heat capacity of the polymer in the same nanocomposite measured using the conventional DSC from our previous study[69] is also plotted, as well as the values for neat PS from Figure 1. The absolute C_p of the polystyrene in the nanocomposite are lower than that of the neat polymer in both the glassy and the liquid regimes. We note that the degree to which the heat capacity of the polystyrene in the nanocomposite is depressed will vary if the weight fraction of silica from the TGA measurements is in error; however, for the heat capacity to be equal to the bulk value in the liquid state at 150°C would require the nanocomposite to contain over 30% silica rather than the 20% measured by TGA, a difference that is

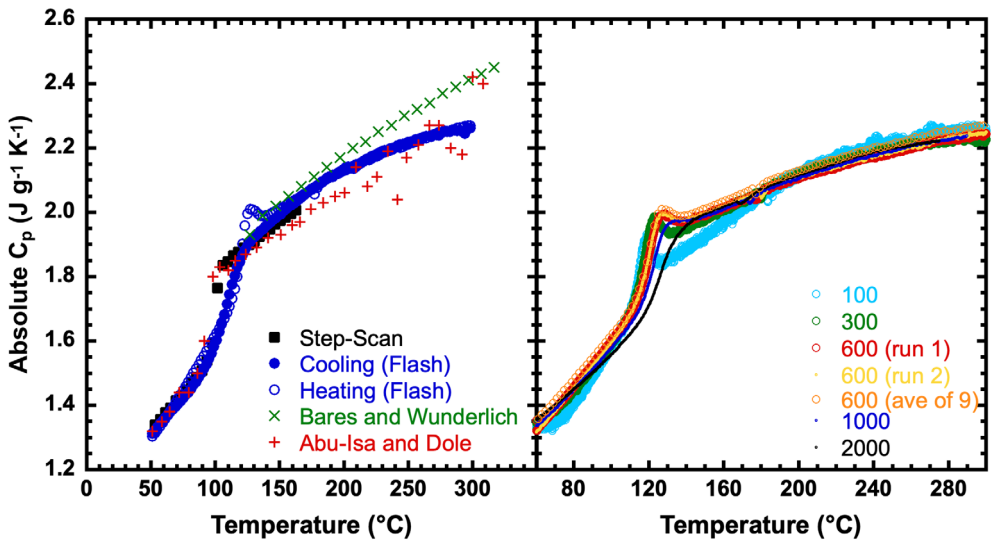

FIGURE 1 Absolute heat capacity of polystyrene vs. temperature. On the left, C_p from Flash obtained at 600 K/s on cooling (blue filled circles) and heating (blue open circles) is plotted showing the average for nine scans going to sequentially higher temperatures. Also shown is data obtained by step scan in previous work (black filled squares),[69] from Bares and Wunderlich (green x),[81] and from Abu-Isa and Dole (red cross).[80] On the right, C_p data obtained on heating is shown as a function of the rate (K/s) used for the symmetry analysis, along with the averaged heating data from the nine sequential scans obtained at 600 K/s that is shown at left.

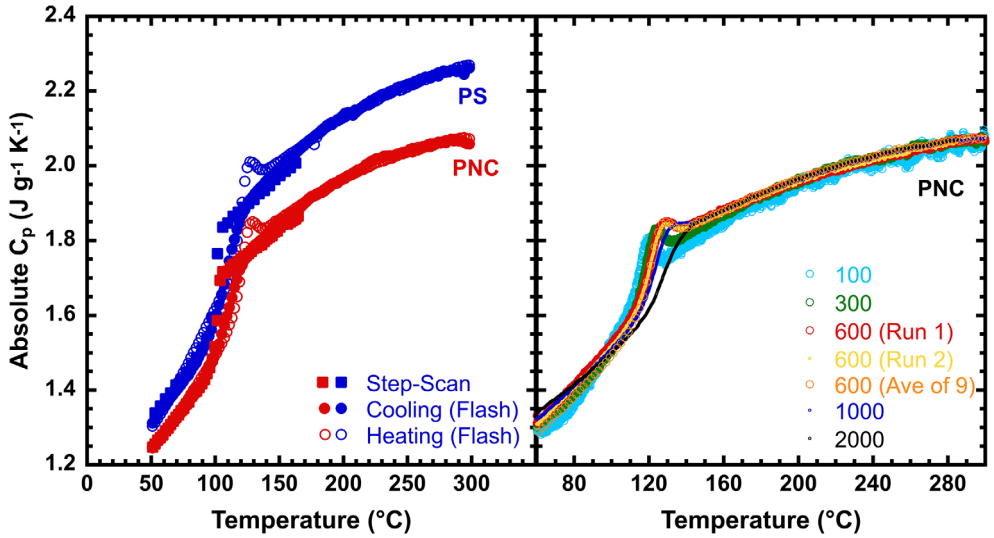

FIGURE 2 Absolute heat capacity versus temperature where heat capacity is normalized per gram polymer with contributions from the silica subtracted for the PNC. On the left, C_p from Flash obtained at 600 K/s on cooling (filled circles) and on heating (open circles) is shown for the nanocomposite PNC (red) and the neat polystyrene PS (blue) showing the average for nine scans going to sequentially higher temperatures; C_p data from step-scan from previous work[69] is also shown as filled squares for both samples. On the right, C_p data on heating for the PNC is shown as a function of the rate (K/s) used for the symmetry analysis, along with the averaged heating data from the nine sequential scans obtained at 600 K/s that is shown at left.

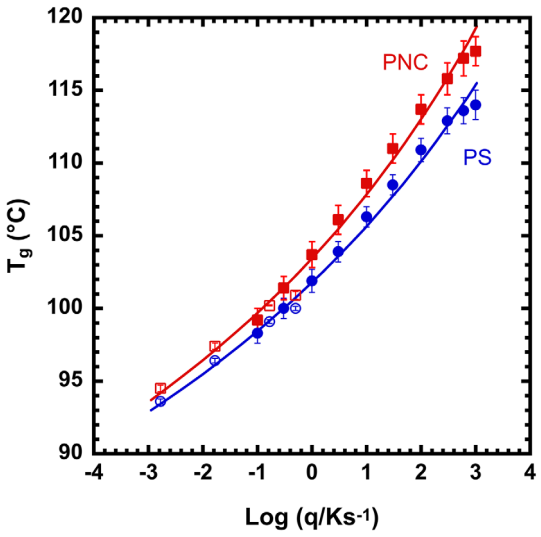

FIGURE 3 Glass transition temperature as a function of the logarithm of the cooling rate for the neat PS (blue circles) and the nanocomposite PNC (red squares), showing values from Flash DSC (filled symbols) and from previous work[69] using conventional DSC (unfilled symbols). The error bars in the flash dash represent the standard deviation of twelve (12) repetitive runs of the same sample. The solid lines represent the WLF fits.

well beyond the error in the measurements. The findings of a depressed heat capacity at high temperatures for the polymer are consistent with our previous study[69] which only went to 170°C, but what is surprising is that there is no indication of C_p of the nanocomposite increasing towards the neat value. The adjusted heat flow results for PNC obtained from the equal cooling/heating rate experiments, shown in Figure 2 (right), again demonstrate excellent superposition (within 0.7%) between repeated runs performed at 600 K/s and also show that the high-temperature flattening observed in the nanocomposite sample also does not depend on the rate of the measurement.

The glass transition temperature of the materials, calculated using the Moynihan's method, are plotted with respect to the logarithm of the cooling rate in Figure 3. Also plotted in Figure 3 are the glass transition temperatures of the materials measured using the conventional DSC in our previous work.[69] Six decades of cooling rates are covered, from 0.0017 K/s up to 1000 K/s considering both the conventional and the Flash DSC runs, in which the conventional DSC values were obtained at cooling rates from 0.0017 K/s (0.1 K/min) up to 0.5 K/s (30 K/min) and the Flash DSC values were obtained at cooling rates from 0.1 K/s up to 1000 K/s. Interestingly, the T_g difference between the neat and the nanocomposite samples increases with increasing cooling rate. This is the opposite of what is generally observed for nanoconfined samples where no significant change in T_g is observed at the highest rates and the T_g depression increases with decreasing cooling rate.[89,90] Here, we report a T_g elevation that is 4 ± 1 K at 1000 K/s and only 1 to 2 K at the rates used in the conventional DSC.[69] Our results are within the range of those reported in the literature for the glass transition temperature for polystyrene-grafted silica nanoparticles, where T_g generally increases from

1 to 13 K over the value of the neat system of similar molecular weight, with larger increases reported for shorter chains and higher grafting densities.[73,91–94] Similarly, modest increases in T_g have been reported for polyisoprene-grafted silica nanoparticles,[95] whereas for poly(methyl acrylate)-grafted Si, no change in T_g was observed for the nanocomposites with the longest grafts and about a 12 or 13 K increase was observed for the nanocomposite having the shortest grafts.[96] Interestingly, the increase in T_g for matrix-free hairy nanoparticles is reported to be insensitive to graft density by Archer et al.,[95] leading them to suggest that the increase in T_g is associated with entropy losses due to space-filling constraints, and our data support this argument.[69]

The cooling rate-dependent T_g values are fitted using the Williams-Landel-Ferry (WLF) equation:[97]

$$\log\frac{q_{ref}}{q}=\frac{-C_1\left(T_g-T_{g,ref}\right)}{C_2+\left(T_g-T_{g,ref}\right)} \quad (4)$$

where q is the cooling rate, q_{ref} is the cooling rate at which $T_g = T_{g,ref}$, and C_1 and C_2 are fitting parameters. Meanwhile, the temperature dependence of the relaxation time in the vicinity of the glass transition, also known as the fragility (m), is calculated using Equation (5):[98]

$$m=-\frac{d\log q}{d\left(\frac{T_{g,ref}}{T_g}\right)}=T_g\frac{C_1}{C_2} \quad (5)$$

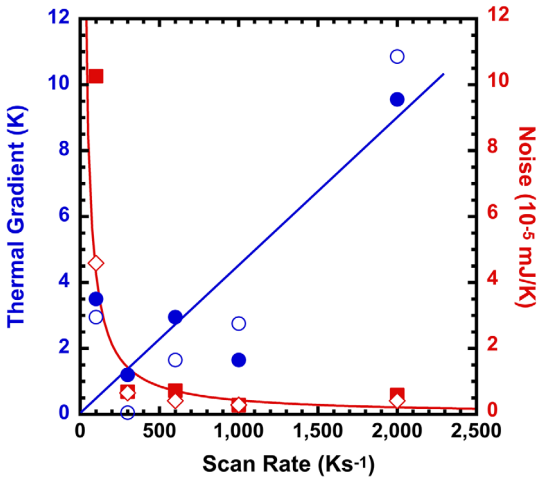

FIGURE 4 Thermal gradient as a function of scan rate (left y-axis, blue) as obtained from half the difference in T_g on cooling and subsequent heating scans and noise in heat capacity as a function of scan rate (right y-axis, red) for neat PS (filled symbols) and PNC (open symbols). Lines shown are a linear fit (thermal gradient) and linear with reciprocal scan rate (noise).

Fragility values of 111 and 100 are calculated for neat and nanocomposite systems, respectively, at 0.1 K/s T_g indicating little if any difference between the two systems similar to our previous work and consistent with the literature.[38,69,73] We note that our values are approximately 10% and 19% lower than the values obtained for the same materials using rheology in our previous work[69] and the neat polystyrene value is also 10% lower than other reports of bulk polystyrene studied using the Flash DSC.[89,90] We attribute these discrepancies to the difference in experimental time windows between rheological and calorimetric measurements (12 vs. 6 decades) in addition to the uncertainties in fragility measurements, of about 10%–15%.[98]

4 | DISCUSSION

The dynamic temperature gradient in the Flash DSC samples is equated to half of the difference in T_g measured on cooling and a subsequent heating run performed at the same rate, as suggested by Schawe.[87] The temperature gradient increases approximately linearly with scan rate, as shown in Figure 4, with values ranging from 0 to 1 K for a scan rate of 300 K/s to as high as 10 K at a scan rate of 2000 K/s. The temperature gradient obtained at 100 K/s is higher than expected presumably due to the higher noise associated in the heat flow at that rate resulting in inaccurate determination of T_g. Also shown in the same plot is the dependence of the noise in the heat capacity measurement (mJ/K, calculated in a temperature range from 80°C to 100°C). The noise increases with decreasing rate as is linear with reciprocal cooling rate. Hence, the optimum rate for measurements, where both noise and thermal gradients are low, lies between 300 and 1000 K/s for the samples studied here. Of course, the optimum rate will depend on the sample thickness, since the thicker the sample, the larger the thermal gradients at a given rate and the smaller the noise (assuming that the sample area remains constant).

The presence of an immobile glassy layer around the nanoparticles is based on the findings in our previous work[69] where, for the same nanocomposite system, we reported a decrease in the magnitude of ΔC_p at T_g for the nanocomposite as compared to the corresponding neat polymer, even after removing the contribution of the silica (i.e., normalizing for the amount of polymer present). To further examine the Flash DSC data for the presence or absence of the additional step change at high temperatures, corresponding to the mobilization of the "immobile" layer, the derivatives of the absolute heat capacity of PNC and the corresponding neat PS are calculated with respect to temperature and plotted in Figure 5. On the scale shown, the T_g difference (of 2 K) is not observable,

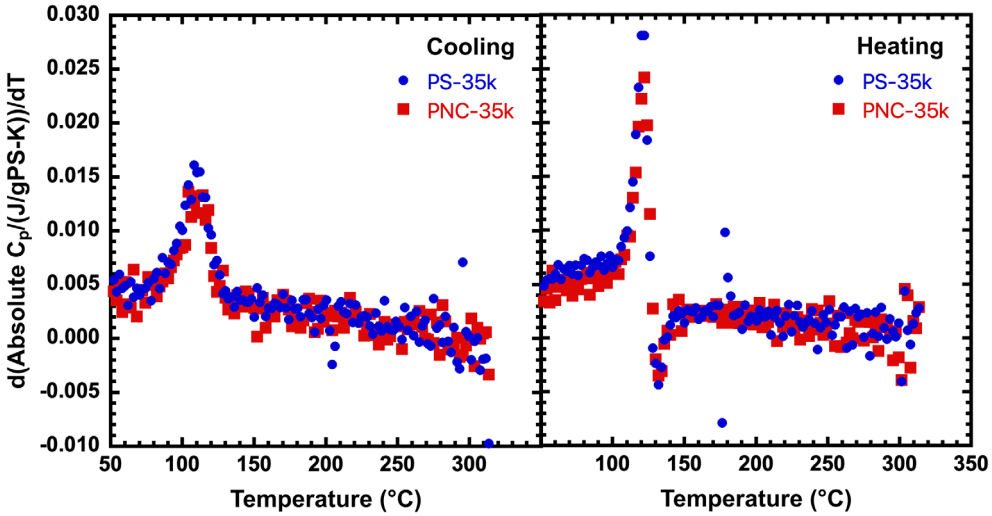

FIGURE 5 Derivative of the absolute heat capacity with respect to temperature for nanocomposite PNC (red squares) and neat PS (blue circles) for data obtained on cooling (left) and on heating (right). The absolute heat capacity is per gram polymer with contributions from the silica subtracted for the PNC

and the temperature dependences of the glass and liquid heat capacities (dC_p/dT) of both samples are the same within the scatter of the data. The neat sample has slightly more area under the peak associated with the glass transition, which reflects its larger value of ΔC_p. There is no indication of any additional relaxation step indicative of mobilization of the immobile glassy layer for the nanocomposite sample in the temperature range investigated. This is consistent with a study of PDMS matrix-free grafted nanoparticles that attempted to examine the interfacial dynamics of the immobile or rigid layer using broadband dielectric spectroscopy,[32] as well as PI-grafted nanocomposites,[37] but PDVP-grafted systems show an interfacial relaxation.[35] The differences in these systems may be related, in part, to the strength of the polymer-nanoparticle interaction, with PDVP interacting strongly with silica and PS and PDMS showing hydrophobic interactions. In addition to the effects of polymer/particle interaction strength on the interfacial relaxation, it is also necessary for future work to examine variables such as graft density and graft molecular weight since these influence chain packing and stretching at the nanoparticle surface and, thus, are anticipated to also affect interfacial relaxation.

5 | CONCLUSION

The absolute heat capacity of a matrix-free polystyrene grafted silica nanocomposite system is investigated using ultrafast nanocalorimetry, and results are compared on a per gram polymer basis to a neat polystyrene sample of similar molecular weight. The absolute heat capacity of the matrix-free nanocomposite is found to neither reach the values of the analogous neat polymer nor to show additional relaxations at high temperatures that could be attributable to the mobilization of the glassy "immobile" polymer layer at the nanoparticle surface. Moreover, the cooling rate dependence of the glass transition temperature is studied for both systems. The T_g data of the nanocomposite is higher than that of the neat PS, consistent with our previous study[69] using the conventional DSC, and the elevation increases with increasing cooling rate, being 4 ± 1 K at 1000 K/s. The fragility of the nanocomposite is 10% lower than that of the neat polystyrene. The dynamic temperature gradients of the Flash DSC samples are also investigated and found to increase linearly with scan rate, whereas the noise in the C_p measurements increases linearly with reciprocal scan rate.

ACKNOWLEDGMENT

Funding from NSF DMR–2004960 and NSF DMR–2141221 is acknowledged.

DATA AVAILABILITY STATEMENT

Data will be supplied upon reasonable request; email slsimon@ncsu.edu.

ORCID

Yung P. Koh https://orcid.org/0000-0001-5140-1865
Sindee L. Simon https://orcid.org/0000-0001-7498-2826

REFERENCES

[1] R. A. Vaia, J. F. Maguire, *Chem. Mater.* **2007**, *19*(11), 2736.
[2] L. S. Schadler, S. K. Kumar, B. C. Benicewicz, S. L. Lewis, S. E. Harton, *MRS Bull.* **2007**, *32*(4), 335.
[3] S. K. Kumar, R. Krishnamoorti, *Annu. Rev. Chem. Biomol. Eng.* **2010**, *1*, 37.
[4] J. Jancar, J. F. Douglas, F. W. Starr, S. K. Kumar, P. Cassagnau, A. J. Lesser, S. S. Sternstein, M. J. Buehler, *Polymer* **2010**, *51*(15), 3321.

[5] N. J. Fernandes, H. Koerner, E. P. Giannelis, R. A. Vaia, *MRS Communications* **2013**, *3*(1), 13.
[6] Y. Li, T. M. Krentz, L. Wang, B. C. Benicewicz, L. S. Schadler, *ACS Appl. Mater. Interfaces* **2014**, *6*(9), 6005.
[7] S. K. Kumar, B. C. Benicewicz, R. A. Vaia, K. I. Winey, *Macromolecules* **2017**, *50*(3), 714.
[8] R. Sengupta, S. Chakraborty, S. Bandyopadhyay, S. Dasgupta, R. Mukhopadhyay, K. Auddy, A. S. Deuri, *Poly. Eng. Sci.* **2007**, *47*(11), 1956.
[9] M. Aslam, M. A. Kalyar, Z. A. Raza, *Poly. Eng. Sci.* **2018**, *58*(12), 2119.
[10] F. Faridirad, S. Ahmadi, M. Barmar, *Poly. Eng. Sci.* **2017**, *57*(5), 475.
[11] F. W. Starr, T. B. Schrøder, S. C. Glotzer, *Macromolecules* **2002**, *35*(11), 4481.
[12] G. J. Papakonstantopoulos, K. Yoshimoto, M. Doxastakis, P. F. Nealey, J. J. de Pablo, *Phys. Rev. E* **2005**, *72*(3), 031801.
[13] S. Merabia, P. Sotta, D. R. Long, *Macromolecules* **2008**, *41*(21), 8252.
[14] L. Chen, K. Zheng, X. Tian, K. Hu, R. Wang, C. Liu, Y. Li, P. Cui, *Macromolecules* **2010**, *43*(2), 1076.
[15] C. Chevigny, N. Jouault, F. Dalmas, F. Boué, J. Jestin, *J. Polym. Sci., Part B: Polym. Phys.* **2011**, *49*(11), 781.
[16] S. Y. Kim, K. S. Schweizer, C. F. Zukoski, *Phys. Rev. Lett.* **2011**, *107*(22), 225504.
[17] M. Mortezaei, M. H. N. Famili, M. Kokabi, *Compos Sci Technol* **2011**, *71*(8), 1039.
[18] M. Mortezaei, G. Farzi, M. R. Kalaee, M. Zabihpoor, *J. Appl. Polym. Sci.* **2011**, *119*(4), 2039.
[19] B. A. P. Betancourt, J. F. Douglas, F. W. Starr, *Soft Matter* **2013**, *9*(1), 241.
[20] A. Ghanbari, M. Rahimi, J. Dehghany, *J. Phys. Chem. C* **2013**, *117*(47), 25069.
[21] G. Kritikos, A. F. Terzis, *Eur. Polym. J.* **2013**, *49*(3), 613.
[22] B. Natarajan, Y. Li, H. Deng, L. C. Brinson, L. S. Schadler, *Macromolecules* **2013**, *46*(7), 2833.
[23] P. Klonos, A. Kyritsis, P. Pissis, *Eur. Polym. J.* **2015**, *70*, 342.
[24] Y. Lin, L. Liu, G. Xu, D. Zhang, A. Guan, G. Wu, *J. Phys. Chem. C* **2015**, *119*(23), 12956.
[25] A. P. Holt, V. Bocharova, S. Cheng, A. M. Kisliuk, B. T. White, T. Saito, D. Uhrig, J. P. Mahalik, R. Kumar, A. E. Imel, T. Etampawala, H. Martin, N. Sikes, B. G. Sumpter, M. D. Dadmun, A. P. Sokolov, *ACS Nano* **2016**, *10*(7), 6843.
[26] F. W. Starr, J. F. Douglas, D. Meng, S. K. Kumar, *ACS Nano* **2016**, *10*(12), 10960.
[27] B. Carroll, S. Cheng, A. P. Sokolov, *Macromolecules* **2017**, *50*(16), 6149.
[28] S. Cheng, B. Carroll, W. Lu, F. Fan, J.-M. Y. Carrillo, H. Martin, A. P. Holt, N.-G. Kang, V. Bocharova, J. W. Mays, B. G. Sumpter, M. D. Dadmun, A. P. Sokolov, *Macromolecules* **2017**, *50*(6), 2397.
[29] P. Klonos, A. Kyritsis, L. Bokobza, V. M. Gun'ko, P. Pissis, *Colloids Surf., A* **2017**, *519*, 212.
[30] N. Begam, N. Das, S. Chandran, M. Ibrahim, V. Padmanabhan, M. Sprung, J. Basu, *Soft Matter* **2018**, *14*(43), 8853.
[31] A.-C. Genix, V. Bocharova, B. Carroll, M. Lehmann, T. Saito, S. Krueger, L. He, P. Dieudonné-George, A. P. Sokolov, J. Oberdisse, *ACS Appl. Mater. Interfaces* **2019**, *11*(19), 17863.
[32] P. A. Klonos, O. V. Goncharuk, E. M. Pakhlov, D. Sternik, A. Deryło-Marczewska, A. Kyritsis, V. M. Gun'ko, P. Pissis, *Macromolecules* **2019**, *52*(7), 2863.
[33] T. V. Ndoro, M. C. Böhm, F. Müller-Plathe, *Macromolecules* **2012**, *45*(1), 171.
[34] W. You, W. Cui, W. Yu, *Polymer* **2021**, *213*, 123323.
[35] T. Wei, J. M. Torkelson, *Macromolecules* **2020**, *53*(19), 8725.
[36] B. K. Khatiwada, F. D. Blum, *Langmuir* **2019**, *35*(35), 11482.
[37] Y. Lin, S. Hu, G. Wu, *J Phys Chem C* **2019**, *123*(11), 6616.
[38] A. P. Holt, C. Roland, *Soft Matter* **2018**, *14*(42), 8604.
[39] A.-C. Genix, V. Bocharova, A. Kisliuk, B. Carroll, S. Zhao, J. Oberdisse, A. P. Sokolov, *ACS Appl. Mater. Interfaces* **2018**, *10*(39), 33601.
[40] F. Ma, B. Xu, Y. Song, Q. Zheng, *RSC Adv.* **2018**, *8*(56), 31972.
[41] P. Klonos, Y. Bolbukh, C. Koutsiara, K. Zafeiris, O. Kalogeri, D. Sternik, A. Deryło–Marczewska, V. Tertykh, P. Pissis, *Polymer* **2018**, *148*, 1.
[42] S. Koutsoumpis, K. N. Raftopoulos, O. Oguz, C. M. Papadakis, Y. Z. Menceloglu, P. Pissis, *Soft Matter* **2017**, *13*(26), 4580.
[43] G. P. Baeza, C. Dessi, S. Costanzo, D. Zhao, S. Gong, A. Alegria, R. H. Colby, M. Rubinstein, D. Vlassopoulos, S. K. Kumar, *Nat. Commun.* **2016**, *7*, 11368.
[44] S. Cheng, A. P. Holt, H. Wang, F. Fan, V. Bocharova, H. Martin, T. Etampawala, B. T. White, T. Saito, N.-G. Kang, M. D. Dadmun, J. W. Mays, A. P. Sokolov, *Phys. Rev. Lett.* **2016**, *116*(3), 038302.
[45] Z. Zheng, Y. Song, R. Yang, Q. Zheng, *Langmuir* **2015**, *31*(50), 13478.
[46] A. P. Holt, P. J. Griffin, V. Bocharova, A. L. Agapov, A. E. Imel, M. D. Dadmun, J. R. Sangoro, A. P. Sokolov, *Macromolecules* **2014**, *47*(5), 1837.
[47] M. M. Kummali, L. A. Miccio, G. A. Schwartz, A. Alegría, J. Colmenero, J. Otegui, A. Petzold, S. Westermann, *Polymer* **2013**, *54*(18), 4980.
[48] A. P. Holt, J. R. Sangoro, Y. Wang, A. L. Agapov, A. P. Sokolov, *Macromolecules* **2013**, *46*(10), 4168.
[49] A. Papon, H. Montes, F. Lequeux, J. Oberdisse, K. Saalwaechter, L. Guy, *Soft Matter* **2012**, *8*(15), 4090.
[50] D. Fragiadakis, L. Bokobza, P. Pissis, *Polymer* **2011**, *52*(14), 3175.
[51] C. G. Robertson, M. Rackaitis, *Macromolecules* **2011**, *44*(5), 1177.
[52] R. Ruggerone, V. R. Geiser, S. Dalle Vacche, Y. Leterrier, J.-A. E. Manson, *Macromolecules* **2010**, *43*(24), 10490.
[53] S. E. Harton, S. K. Kumar, H. Yang, T. Koga, K. Hicks, H. Lee, J. Mijovic, M. Liu, R. S. Vallery, D. W. Gidley, *Macromolecules* **2010**, *43*(7), 3415.
[54] D. Fragiadakis, P. Pissis, *J. Non-Cryst. Solids* **2007**, *353*(47–51), 4344.
[55] I. Popov, B. Carroll, V. Bocharova, A.-C. Genix, S. Cheng, A. Khamzin, A. Kisliuk, A. P. Sokolov, *Macromolecules* **2020**, *53*(10), 4126.
[56] A. P. Holt, V. Bocharova, S. Cheng, A. M. Kisliuk, G. Ehlers, E. Mamontov, V. N. Novikov, A. P. Sokolov, *Phys. Rev. Mater.* **2017**, *1*(6), 062601.
[57] Y. Lin, L. Liu, D. Zhang, Y. Liu, A. Guan, G. Wu, *Soft Matter* **2016**, *12*(41), 8542.
[58] G. P. Baeza, J. Oberdisse, A. Alegria, K. Saalwächter, M. Couty, A.-C. Genix, *Polymer* **2015**, *73*, 131.
[59] S. Gong, Q. Chen, J. F. Moll, S. K. Kumar, R. H. Colby, *ACS Macro Lett.* **2014**, *3*(8), 773.

[60] M. Füllbrandt, P. J. Purohit, A. Schönhals, *Macromolecules* **2013**, *46*(11), 4626.
[61] C. Mark, O. Holderer, J. Allgaier, E. Hubner, W. Pyckhout-Hintzen, M. Zamponi, A. Radulescu, A. Feoktystov, M. Monkenbusch, N. Jalarvo, D. Richter, *Phys. Rev. Lett.* **2017**, *119*(4), 047801.
[62] T. Glomann, G. Schneider, J. Allgaier, A. Radulescu, W. Lohstroh, B. Farago, D. Richter, *Phys. Rev. Lett.* **2013**, *110*(17), 178001.
[63] S. Y. Kim, H. W. Meyer, K. Saalwächter, C. F. Zukoski, *Macromolecules* **2012**, *45*(10), 4225.
[64] A. Papon, K. Saalwächter, K. Schäler, L. Guy, F. Lequeux, H. Montes, *Macromolecules* **2011**, *44*(4), 913.
[65] J. Berriot, H. Montes, F. Lequeux, D. Long, P. Sotta, *Macromolecules* **2002**, *35*(26), 9756.
[66] Y. Golitsyn, G. J. Schneider, K. Saalwächter, *J. Chem. Phys.* **2017**, *146*(20), 203303.
[67] J. Berriot, F. Lequeux, L. Monnerie, H. Montes, D. Long, P. Sotta, *J. Non-Cryst. Solids* **2002**, *307*, 719.
[68] V. R. Geiser, Y. Leterrier, J.-A. E. Månson, *Macromolecules* **2010**, *43*(18), 7705.
[69] N. Sakib, Y. P. Koh, Y. Huang, K. I. S. Mongcopa, A. N. Le, B. C. Benicewicz, R. Krishnamoorti, S. L. Simon, *Macromolecules* **2020**, *53*(6), 2123.
[70] P. Klonos, C. Pandis, S. Kripotou, A. Kyritsis, P. Pissis, *IEEE Trans. Dielectr. Electr. Insul.* **2012**, *19*(4), 1283.
[71] R. Tao, S. L. Simon, *J. Polym. Sci., Part B: Polym. Phys.* **2015**, *53*(9), 621.
[72] A. Sargsyan, A. Tonoyan, S. Davtyan, C. Schick, *Eur. Polym. J.* **2007**, *43*(8), 3113.
[73] S. Askar, L. Li, J. M. Torkelson, *Macromolecules* **2017**, *50*(4), 1589.
[74] Y. Li, H. Ishida, H., *Macromolecules* **2005**, *38*, 6513.
[75] D. Kim, S. Srivastava, S. Narayanan, L. A. Archer, *Soft Matter* **2012**, *8*(42), 10813.
[76] A. Papon, H. Montes, M. Hanafi, F. Lequeux, L. Guy, K. Saalwächter, *Phys. Rev. Lett.* **2012**, *108*(6), 065702.
[77] S. Cheng, S. Mirigian, J.-M. Y. Carrillo, V. Bocharova, B. G. Sumpter, K. S. Schweizer, A. P. Sokolov, *J. Chem. Phys.* **2015**, *143*(19), 194704.
[78] J. H. Flynn, in *Handbook of Thermal Analysis and Calorimetry: Applications to Polymers and Plastics*. (Ed: Stephen Z.D. Cheng), Elsevier Science B.V., Amsterdam, Netherlands **2002**, Ch.14.
[79] U. Gaur, *V: Polystyrene.* **1982**, *11*, 313.
[80] I. Abu-Isa, M. Dole, *J. Phys. Chem.* **1965**, *69*(8), 2668.
[81] V. Bares, B. Wunderlich, *J. Polym. Sci., Polym. Phys. Ed.* **1973**, *11*(5), 861.
[82] P. Cebe, B. P. Partlow, D. L. Kaplan, A. Wurm, E. Zhuravlev, C. Schick, *Thermochim. Acta* **2015**, *615*, 8.
[83] P. Cebe, B. P. Partlow, D. L. Kaplan, A. Wurm, E. Zhuravlev, C. Schick, *Acta Biomater.* **2017**, *55*, 323.
[84] M. R. Pallaka, D. K. Unruh, S. L. Simon, *Thermochim. Acta* **2018**, *663*, 157.
[85] C. R. Quick, J. E. K. Schawe, P. J. Uggowitzer, S. Pogatscher, *Thermochim. Acta* **2019**, *677*, 12.
[86] P. Badrinarayanan, W. Zheng, Q. Li, S. L. Simon, *J. Non-Cryst. Solids* **2007**, *353*(26), 2603.
[87] J. E. Schawe, *Thermochim. Acta* **2015**, *603*, 128.
[88] P. J. Linstrom, W. Mallard, NIST Chemistry webbook; NIST standard reference database. **2001**, *69*.
[89] S. Gao, Y. P. Koh, S. L. Simon, *Macromolecules* **2013**, *46*(2), 562.
[90] Y. P. Koh, S. L. Simon, *Polymer* **2018**, *143*, 40.
[91] D. A. Savin, J. Pyun, G. D. Patterson, T. Kowalewski, K. Matyjaszewski, *J. Polym. Sci. Pol. Phys.* **2002**, *40*(23), 2667.
[92] A. Dang, C. M. Hui, R. Ferebee, J. Kubiak, T. H. Li, K. Matyjaszewski, M. R. Bockstaller, *Macromol. Symp.* **2013**, *331-332*(1), 9.
[93] H. Koerner, E. Opsitnick, C. A. Grabowski, L. F. Drummy, M. S. Hsiao, J. Che, M. Pike, V. Person, M. R. Bockstaller, J. S. Meth, R. A. Vaia, *J. Polym. Sci. Pol. Phys.* **2016**, *54*(2), 319.
[94] Y. Cang, A. N. Reuss, J. Lee, J. J. Yan, J. N. Zhang, E. Alonso-Redondo, R. Sainidou, P. Rembert, K. Matyjaszewski, M. R. Bockstaller, G. Fytas, *Macromolecules* **2017**, *50*(21), 8658.
[95] S. A. Kim, R. Mangal, L. A. Archer, *Macromolecules* **2015**, *48*(17), 6280.
[96] C. R. Bilchak, E. Buenning, M. Asai, K. Zhang, C. J. Durning, S. K. Kumar, Y. C. Huang, B. C. Benicewicz, D. W. Gidley, S. W. Cheng, A. P. Sokolov, M. Minelli, F. Doghieri, *Macromolecules* **2017**, *50*(18), 7111.
[97] M. L. Williams, R. F. Landel, J. D. Ferry, *J. Am. Chem. Soc.* **1955**, *77*(14), 3701.
[98] R. Tao, E. Gurung, M. M. Cetin, M. F. Mayer, E. L. Quitevis, S. L. Simon, *Thermochim. Acta* **2017**, *654*, 121.

How to cite this article: N. Sakib, Y. P. Koh, S. L. Simon, *Polym. Eng. Sci.* **2022**, *62*(9), 2977. https://doi.org/10.1002/pen.26078